

The chromium position in ruby

By S. C. MOSS and R. E. NEWNHAM

Massachusetts Institute of Technology, Cambridge, Mass.

With 1 figure

(Received March 18, 1964)

Auszug

Die Lage von Chromionen in hochdotierten Rubinkristallen wurde aus den $00\cdot l$ -Intensitäten ermittelt. Cr befindet sich an einer Gitterstelle, die um $0,06 \text{ \AA}$ von der normalen Aluminiumlage entfernt ist. Im Widerspruch zu den neuesten Kristallfeldberechnungen ist es in der Richtung auf den nächsten Al-Nachbarn verschoben, wodurch die kleinsten Metall–Wasserstoff-Entfernungen vergrößert werden.

Abstract

The chromium position in highly doped ruby has been determined from $00\cdot l$ intensity data. Cr occupies a site 0.06 \AA from the normal Al position. Contrary to recent crystal-field calculations, the shift is towards the nearest Al neighbor, increasing the smaller metal–oxygen distances.

Interest in ruby-maser devices has prompted many investigations of the $\text{Al}_{2-2x}\text{Cr}_{2x}\text{O}_3$ solid-solution series. Several recent publications^{1–3} suggest that the chromium site in ruby is slightly displaced from the position normally occupied by Al. This paper reports an x-ray determination of the Cr coordinate in highly doped ruby.

Indirect evidence for the Cr shift comes from ENDOR experiments and from optical absorption data. Electron-nuclear double resonance (ENDOR) experiments combine electron spectroscopy with radio-frequency nuclear resonance. In ruby the magnetic dipole and electric quadrupole moments of the Al nuclei interact with the unpaired

¹ N. LAURANCE, E. C. McIRVINE and J. LAMBE, Aluminum hyperfine interactions in ruby. *J. Physic. Chem. Solids* **23** (1962) 515–531.

² D. S. McCLURE, Optical spectra of transition-metal ions in corundum. *J. Chem. Physics* **36** (1962) 2757–2779.

³ L. L. LOHR and W. N. LIPSCOMB, Molecular orbital theory of spectra of Cr^{3+} ions in crystals. *J. Chem. Physics* **38** (1963) 1607–1612.

electrons of chromium. Based on a simplified model, the quadrupole interactions observed in ruby were explained assuming a Cr displacement of 0.2 Å along c , away from the nearest cation neighbor¹. A shift in the same direction was proposed by McCLURE² in interpreting the ruby crystal-field spectra. Point-charge model calculations of the trigonal-field parameter agree best with experiment when a 0.1 Å displacement is introduced. LCAO—MO calculations by LOHR and LIPSCOMB³ led to a similar conclusion.

The oxygen positions in ruby approximate hexagonal close packing, with trivalent aluminum and chromium occupying two thirds of the octahedral interstices. The space group is $R\bar{3}c$ with six formula units in the hexagonal unit cell. Lattice parameters for $\text{Al}_{1.92}\text{Cr}_{0.08}\text{O}_3$, the composition used in this study, are $a = 4.7686$, $c = 13.018$ Å, about 0.2% larger than those of pure corundum⁴ ($a = 4.7589$, $c = 12.991$ Å). The oxygen atoms are located in special positions along the two-fold axes at $\pm (w, 0, \frac{1}{4}; 0, w, \frac{1}{4}; \bar{w}, \bar{w}, \frac{1}{4})$ and metal ions lie on three-fold axes at $\pm (0, 0, z; 0, 0, \frac{1}{2} + z)$; z_{Cr} and z_{Al} were determined for 4% ruby using accurate $00\cdot l$ counter data.

Intensity measurements on large ruby plates in reflection position were made using a motor-driven spectrometer and an open counter slit. Monochromatic $\text{MoK}\alpha$ radiation was obtained with a bent silicon crystal cut parallel to (111), thereby eliminating $\lambda/2$; $\lambda/3$ was eliminated by operating the x-ray tube at 31 kV. Periodic monitoring showed that the incident-beam intensity drifted by less than 1%. Very narrow horizontal and vertical entrance slits confined the x-ray beam to the specimen surface and gave a rocking half width of only six minutes in θ for a NaCl 200 reflection.

Polished corundum and ruby plates 1 cm² in area were mounted on a two-circle goniometer, collinear with the spectrometer axis. The (00·1) plates were cut from single-crystal Verneuil boules grown by Dr. A. LINZ, E. F. FARRELL and A. VETROVS, Laboratory for Insulation Research, M.I.T. After aligning the crystals so that [00·1] and the diffraction vector were parallel to within five minutes of arc, the $00\cdot l$ intensities were recorded at maximum sensitivity using a drive speed of $\frac{1}{6}^\circ \theta$ per minute. The detector was set at the midpoint of each reflection, and the scintillation-counter slit opened to accept a diffracted beam over $1.75^\circ \theta$, about 0.5° larger than the broadest ruby reflection. Small absorption errors arising from surface misorien-

⁴ A. LINZ, JR., and R. E. NEWNHAM, Ultraviolet absorption spectra in ruby. *Physic. Rev.* **123** (1961) 500—501.

tation were eliminated by averaging the integrated intensities for the 0° and 180° positions related by rotation about $[00\cdot 1]$. The estimated accuracy of the $00\cdot l$ integrated intensities given in Table 1 is 3%. Intensities for two ruby plates cut from the same boule (*A* and *B*, Table 1) provide a measure of the reproducibility. Due consideration

Table 1. Summary of $|F_o|^2$ values, corrected for polarization and absorption

$h k \cdot l$	Al ₂ O ₃	4% Ruby			Ratio Ruby/Al ₂ O ₃
		Crystal A	Crystal B	Average	
0 0 · 6	2205	1217	1259	1238	0.56 ± .01
0 0 · 12	18524	21652	20910	21281	1.15 ± .02
0 0 · 18	16968	18032	16550	17291	1.02 ± .04
0 0 · 24	279	399	322	361	1.29 ± .13
0 0 · 30	7543	8592	8544	8568	1.13 ± .01

was given to the small differences in absorption coefficient and angular factors in placing the Al₂O₃ and ruby intensities on an identical scale. As with most crystals grown by flame fusion, the specimens were highly strained, minimizing primary extinction. Secondary extinction proved negligible because the observed intensity for $00\cdot 6$, the reflection most likely to be diminished, is larger than the calculated value (Table 2).

Table 2

Comparison of observed and calculated structure factors for corundum and ruby

$h k \cdot l$	00 · 6	00 · 12	00 · 18	00 · 24	00 · 30
Al ₂ O ₃					
$ F_o $	47.0	136.1	130.3	16.7	86.9
F_c ($z_{Al} = .3523$)	-41.6	136.6	-134.7	-16.7	-87.4
4% ruby					
$ F_o $	35.2	145.9	131.5	19.0	92.6
F_c ($z_{Cr} = .347$)	-31.5	142.6	-132.1	-17.3	-90.9
F_c ($z_{Cr} = .352$)	-33.5	138.1	-137.4	-21.2	-91.1
F_c ($z_{Cr} = .360$)	-38.2	130.3	-141.9	-19.0	-83.8

The structure factor for the $00\cdot l$ reflections with $l = 6n$ is given by

$$F_c = 2xf_{Cr} e^{-M_{Cr}} \cos 2\pi lz_{Cr} + 2(1-x)f_{Al} e^{-M_{Al}} \cos 2\pi lz_{Al} + 3 \cos(\pi l/2) f_O e^{-M_O},$$

where the atomic fraction $x = 0$ for corundum, and 0.04 for the ruby specimens. Scattering factors, corrected for dispersion and ionization,

were taken from Vol. III of the *International tables for x-ray crystallography*. The Al_2O_3 intensity data were used in determining the scale factor, temperature factors, and aluminum coordinate. Excellent agreement (Table 2) was obtained with the following values: $z_{\text{Al}} = 0.3523$, $B_{\text{Al}} = 0.14$, and $B_{\text{O}} = 0.22$. A previous refinement based on photographic intensities gave $z_{\text{Al}} = .3520 \pm .0003^5$.

The ruby structure factors (Table 2) were calculated with the B values, z_{Al} , and scale factor derived from the corundum intensity data. When compared with experiment, calculations for various chromium coordinates gave the R -factor graph in Fig. 1, showing

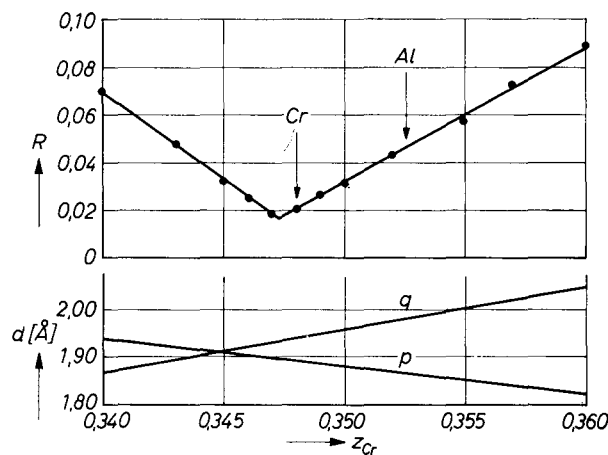


Fig. 1. The R factor and chromium-oxygen distances for 4% ruby plotted as a function of z_{Cr} , the Cr atomic coordinate. q is the distance to the three oxygens shared with the closest Al neighbor, and p represents the distance to the other oxygen triad. Arrows indicate the Al and Cr coordinates derived from the x-ray intensity data

a well-defined minimum near $z_{\text{Cr}} = 0.347$. Comparing intensities rather than structure amplitudes gives a slightly different value of 0.348, about 0.06 Å removed from the Al site. Structure factors calculated for $z_{\text{Cr}} = .360$, the 0.1 Å shift in the opposite direction proposed by McCLURE², gave poor agreement for several reflections (Table 2).

Nearest-neighbor Cr—O distances, plotted as a function of z_{Cr} in Fig. 1, were calculated assuming the oxygens to remain fixed. Our justification for this assumption is the x-ray data just presented and the results of previous refinements⁵ of Al_2O_3 and Cr_2O_3 . The oxygen

⁵ R. E. NEWNHAM and Y. M. DEHAAN, Refinement of the $\alpha\text{Al}_2\text{O}_3$, Ti_2O_3 , V_2O_3 and Cr_2O_3 structures. *Z. Kristallogr.* **117** (1962) 235–237.

parameter is 0.306 ± 0.004 in both end members of the ruby solid-solution series. For $z_{\text{Cr}} = 0.348$, the distance q to the three oxygens shared with the closest Al neighbor is 1.93_8 \AA , and the other three bond lengths p are 1.88_4 \AA . The chromium-oxygen distances in Cr_2O_3 ($q = 2.02$, $p = 1.97$) are about 4% larger and show the same asymmetry, $q-p = .05 \text{ \AA}$. Crystal-field calculations by ORGEL⁶ show that a 4% compression of the normal CrO_6 octahedron shifts the optical absorption bands by an amount sufficient to explain the color of ruby. Most chromium compounds are green, not red. The Al-O distances in corundum and in ruby are $q = 1.97$, $p = 1.86$. In substituting for Al, the larger Cr^{3+} ion chooses a site which will increase the shorter distance, p .

This work was sponsored by the U.S. Air Force, Aeronautical Systems Division, under Contract AF 33 (616)-8353.

⁶ L. E. ORGEL, Ion compression and the colour of ruby. *Nature* [London] **179** (1957) 1348.